Oriented surface-anchored metal–organic frameworks (SurMOFs) as electrochromic thin films

Antoine Mazel, Lucas Rocco, Nicolas Penin, Aline Rougier

ADVANCED OPTICAL MATERIALS
www.advopticalmat.de

Oriented Surface-Anchored Metal–Organic Frameworks (SurMOFs) as Electrochromic Thin Films

*Antoine Mazel, Lucas Rocco, Nicolas Penin, and Aline Rougier**

Novel electrochromic hybrid thin films are synthesized following a liquid-phase epitaxy in a layer-by-layer fashion, yielding highly oriented surface-anchored metal–organic frameworks (SurMOFs). The initial orange color of this $\{Zn_2(PDICl_4)_2\}$ crystalline thin films is reversibly switched by electrochemical reduction. In a lithium-based electrolyte, a dark blue color is obtained in few seconds with a color efficiency of 104.8 $cm^2\ C^{-1}$ ($\lambda = 645$ nm). Interestingly, the color of the reduced state is easily modulated by changing the electrolyte composition. Clearly, two different mechanisms are implicated and the reduced species responsible of the color are identified. Taking advantage of this unusual property, electrochromic devices with a novel configuration are designed leading to an original prototype capable of reversibly switching from a single initial orange color to two different colors simultaneously, namely dark blue and cyan.

1. Introduction

The development of metal–organic frameworks (MOFs) for advanced applications in nanotechnology requires the immobilization of these architectures on surfaces. MOFs can either be grown solvothermally on a surface or coated by different techniques, such as doctor blading or bar-coating, ultimately leading to polycrystalline assemblies where MOFs particles are usually randomly oriented on the surface.[1] More recently, a strategy based on the sequential and controlled immobilization of the key components of the MOFs led to the fabrication of highly homogenous materials where the ligands and the metals present a preferential orientation. These new MOF thin films are called surface-anchored metal–organic frameworks (SurMOFs).[2,3] Besides the generation of highly oriented and noninterpenetrated materials,[4] this method uses a very small amount of precursors (few mg cm^{-2}) making SurMOFs ideal candidates for the integration of highly sophisticated ligands into functional materials.

Owing to their high versatility and infinite combination of metallic centers and organic ligands, SurMOFs are of interest for a very wide range of applications, spanning from photoelectronics, catalysis, water remediation, or solar energy conversion.[5–8] Taking advantage of the highly oriented character of SurMOF, we extended the range of applications by investigating electrochromic properties. Electrochromism (EC) refers to a change of the optical properties of a material upon application of a voltage.[9] This property find applications in smart windows, mirror, or display devices.[10–12] MOFs have already been used in electrochromics,[13–15] in these articles, MOFs were either deposited on surface after synthesis or directly synthesized on the surface with no intention on orienting the growth, leading to polycrystalline materials. To our knowledge, no reports on highly oriented MOF for electrochromism are published to date.

2. Results and Discussion

In this work, SurMOF-2 type of structure was synthesized by using zinc acetate, an electrochemically neutral metal source, and an electrochromic linker. Thus, the electrochromic properties of the SurMOF arise solely from the organic linker. A ligand from the perylene diimide (PDI) family was chosen. These highly colored chromophores exhibit strong stability and excellent electron affinity imparted by the four carbonyl moieties present on the core allowing reduction into stable radical anions and dianions.[16] In addition, reversible redox interactions between Na/Li ions are commonly observed thanks to an enolization process located on the carbonyl groups.[17] All of these features are of extreme importance to achieve efficient and reversible electrochromism. Herein, the bay positions of the PDI were substituted by chlorine atoms, leading to a diminution of its lowest unoccupied molecular orbital level, thus further increasing its electron affinity.[18] In addition, benzoic acids were introduced at the imide position, leading to a ditopic dicarboxylate linker similar to the terephtalic acid.

The orange-colored films of $\{Zn_2(PDICl_4)_2\}$ (**S1**) (**Figure 1**) were grown at room temperature on indium tin

A. Mazel, L. Rocco, N. Penin, A. Rougier
ICMCB (UMR 5026)
CNRS
Bx INP
University of Bordeaux
F-33600 Pessac, France
E-mail: aline.rougier@icmcb.cnrs.fr

The ORCID identification number(s) for the author(s) of this article can be found under https://doi.org/10.1002/adom.202202939.

DOI: 10.1002/adom.202202939

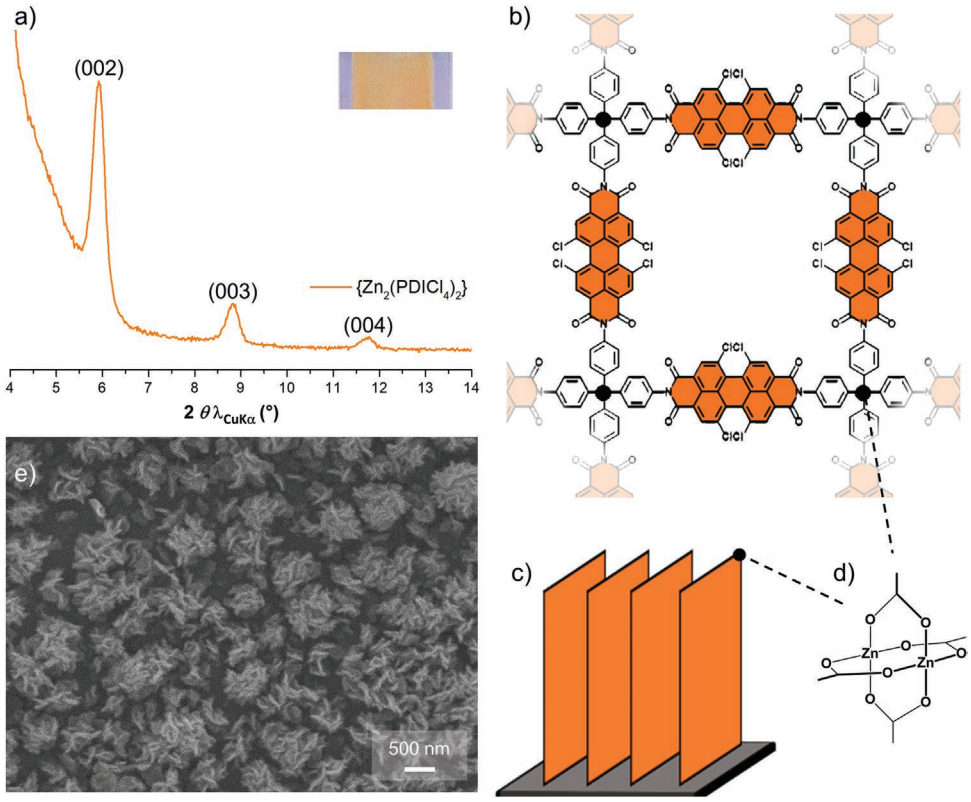

Figure 1. Structure of **S1**. a) Out-of-plane XRD patterns and a photograph of the as deposited film. Illustration of b) the 2D sheets, c) their stacking, and d) the zinc paddlewheel. e) Top view SEM picture.

oxide (ITO)/glass substrates using liquid-phase epitaxy (LPE) in a layer-by-layer (LbL) fashion via spray-coating using zinc acetate as metal source and $PDICl_4$ as organic linker. This method uses highly diluted concentration of ligands and is then particularly suitable for molecules obtained in a few gram scale, usually through multistep synthesis. Thanks to the low concentration of ligands, aggregation was not an issue and ethanol/DMF (95:5) solution could be used. The thickness of the films was controlled by the number of deposition cycles.

The out-of-plane X-ray diffraction (XRD) data revealed highly oriented Zn-SurMOF-2 structure with [00l] orientation (Figure 1a) which is consistent with other SurMOFs obtained from various ditopic dicarboxylate linkers and zinc acetate via LPE methods.[19–22] These structures consist of 2D square grid-like of $PDICl_4$ parallel and perpendicular to the surface, held together by a Zn paddle wheel (Figure 1b–d). These 2D sheets are then stacked in a AA fashion, as expected in a P4 symmetric SurMOF-2 structure. The lattice dimension perpendicular to the substrate ($2\theta\ \lambda_{CuK\alpha}$ = 3.11°, a = 28 Å) closely matches with the length of the linker. Scanning electron microscopy (SEM) top view images show a morphology based on flake-like domains (Figure 1e). The overall thickness was measured by mechanical profilometry. Because of the spray method used for the synthesis a sharp step between the SurMOF and the substrate could not be achieved. To address this issue, perfectly defined holes of 100 × 100 μm^2 were created by ToF-SIM following chlorine signal response. Mechanical profilometry was then performed four times on four different holes in a horizontal and vertical fashion, giving a mean value of 455 nm associated with the 30 cycles (30C) deposition synthesis.

The electrochromic activity of **S1** grown on ITO/glass substrates was recorded in imidazolium-based ionic liquids. **Figure 2**a,e shows the cyclic voltammograms (CV) of the 30C **S1** films cycled at a scan rate of 20 mV s^{-1} between a potential range of –1 to 0.5 V, in a three electrode cells using saturated calomel electrode (SCE) as reference electrode.

In a lithium-based electrolyte **S1** switches reversibly between an orange (λ_{max} = 483 nm) initial state to a dark blue (λ_{max} = 645 nm) reduced state (–0.8 V) (Figure 2b; and Figure S1, Supporting Information). Maximum absorption wavelength of these two optical states was recorded by spectroelectrochemical measurement at 0.5 and –0.8 V, respectively. This study showed the disappearance of the initial state with the appearance of the reduced state, revealing a complete switching process in 14s as supported by chronoamperometry measurements recorded at the blue state maximum absorption wavelength (645 nm) (Figure 2d; and Figure S2, Supporting Information). We noted that the kinetics of the reverse oxidation process seems faster. This observation points in the direction of a nonsymmetrical process regarding lithium diffusion. One of the critical EC property, the coloration efficiency (CE), defined as the change in optical density ΔOD per-unit inserted charge, can be calculated using the following relations, $\Delta OD = \log (T_{ox.}/T_{red.})$, where $T_{ox.}$ and $T_{red.}$ are the transmittance in the oxidized and reduced states, respectively, and CE = ΔOD/Q where Q is the amount of charge transferred per unit area. A coloration efficiency of

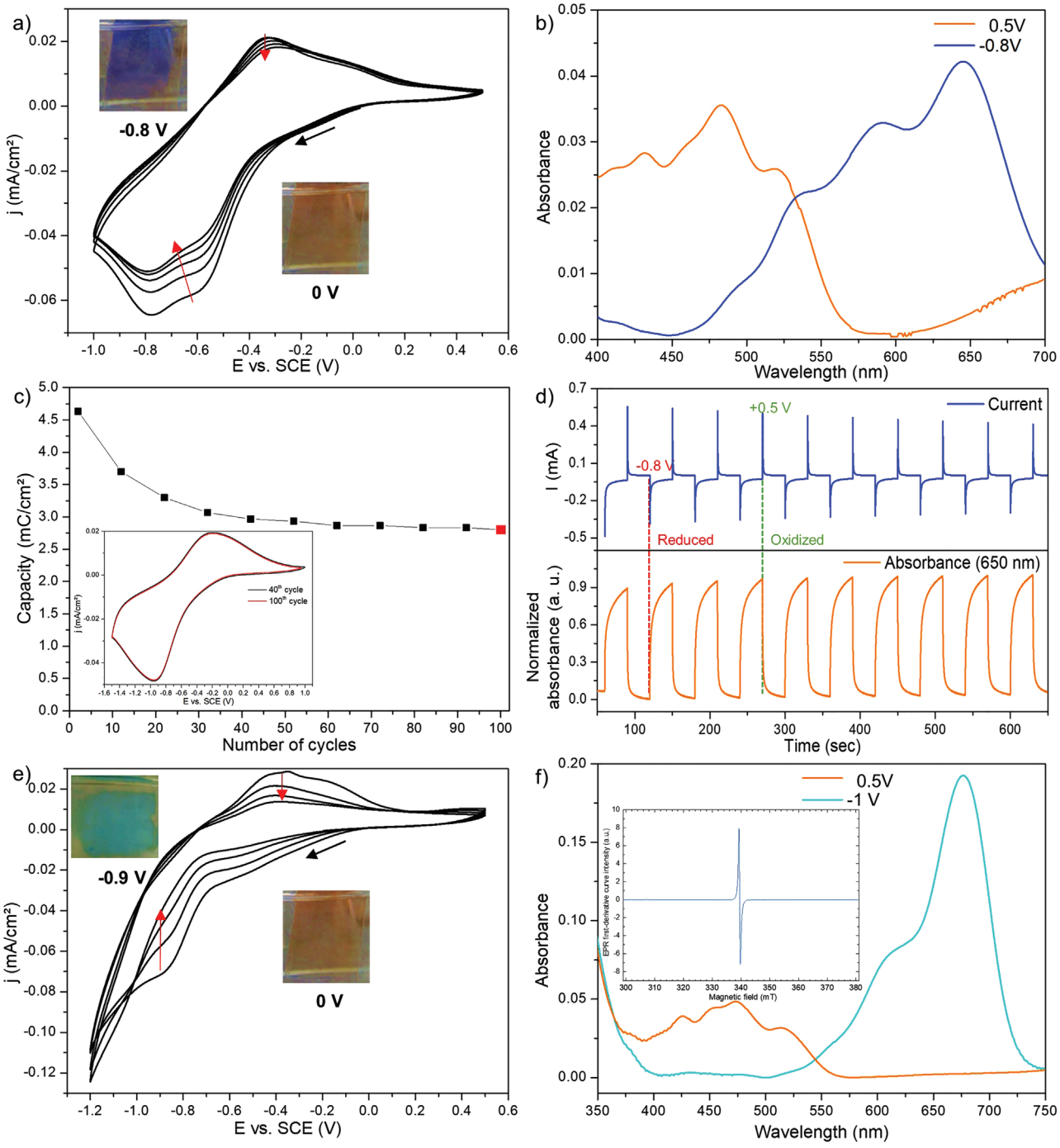

Figure 2. a) Cyclic voltammograms of **S1** in LiTFSI-EMITFSI with picture of the initial state (0 V) and reduced state (–0.8 V) (red arrows pointing from the first cycle to the last). b) Absorption spectra of the as-deposited film and after polarization at –0.8 V in LiTFSI-EMITFSI. c) Charge capacity evolution with the number of cycles as inset, CVs of the 40th and 100th cycle. d) Chronoamperometry (–0.8 and +0.5 V) coupled with absorption spectrum at 645 nm of **S1** in LiTFSI-EMITFSI. e) Cyclic voltammograms of **S1** in EMITFSI with picture of the initial state (0 V) and reduced state (–0.9 V) (red arrows pointing from the first cycle to the last). f) Absorption spectra of **S1** in EMITFSI as-deposited and after polarization at –1 V. As inset, EPR spectrum of reduced **S1** in EMITFSI at 30 K (100 kHz magnetic field modulation of 0.1 mT and a microwave power of 50 mW).

104.8 cm^2 C^{-1} (λ = 645 nm) was calculated (Figure S2, Supporting Information). Similar results were obtained in a sodium-based electrolyte. Those two optical states are consistent with species already identified in literature obtained by chemical reduction in a sodium containing solution of $PDICl_4$ molecules[17,23] pointing in the direction that this color change is mostly due to interactions between Li^+ ions with the $PDICl_4$ radical dianions. After a loss in capacity due probably

to the desorption of noncoordinated linker on the surface, the film shows good stability and reversibility in lithium bis-trifluoromethanesulfonimide in 1-ethyl-3-methylimidazolium bis-(trifluoromethanesulfonyl)-imide (LiTFSI-EMITFSI) as confirmed by the absence of modification of the CV shape (Figure 2c).

Interestingly, in a salt-free ionic liquid electrolyte the switch occurs between the initial orange state to a cyan reduced state (−0.9 V) (Figure 2e). This coloration is due to the formation of free $PDICl_4$ radical dianions as suggested by the value of the wavelength and intensity of the reduced state absorption band recorded during in situ measurement[24] and confirmed by electron paramagnetic resonance, EPR, measurement showing one intense resonance with a g-factor of 2.0045 with no hyperfine coupling (Figure 2f). This result indicates a complete delocalization of unpaired electrons over the ligand structure. However, cycling in EMITFSI leads to a rapid delamination of the SurMOF film after the 1st or 2nd cycle, preventing us at this stage to further characterize the reduced state. After cycling, a cyan film was observed floating next to the ITO surface, in agreement with the featureless absorption spectra observed during in situ measurement, closer from a solution spectra than a solid-state one. The presence of an acidic proton at the C2 position of the imidazolium appears to be responsible for the lack of stability of the SurMOF. After methylation of this position, stability was greatly improved and delamination was no longer observed. This observation is coherent with the known instability of Zn-carboxylate MOFs in acidic medium.

Even though good electrochemical stability was achieved, a loss in the intensity of the (002) and (003) peaks and the disappearance of the (004) peak were observed by XRD after five CV cycles in LiTFSI-EMITFSI (**Figure 3**a). In addition, the so-called electrochemical grinding is mostly responsible for the reduction of the flake-like domain size upon cycling (Figure 3b,c).

It is relevant to note that color dependency on electrolyte composition is an uncommon property in EC materials. Generally, a single material adopts a similar coloration independently of the electrolyte nature, as illustrated by the brownish anodic coloration of NiO films or the bluish cathodic coloration of poly(3,4-ethylenedioxythiophene) polystyrene sulfonate, PEDOT:PSS, cycled in lithium based or small free cations electrolytes.[25,26] Taking advantage of this noteworthy property, a bi-color electrochromic device (ECD) with an original configuration was designed. **S1** was associated with an ITO/glass counter electrode and LiTFSI-EMITFSI and EMITFSI electrolytes within the same device. In order to achieve contact between the two electrodes, the electrolytes were used in a formulation of PMMA/Butanone, spread on each side of 120 µm thick tape to prevent diffusion of Li^+ cations in EMITFSI electrolyte. Vacuum was applied to remove air bubbles and a heating process at 80 °C allowed the evaporation of butanone, transforming the liquid electrolyte into a sticky paste thus creating a conductive hydrophobic membrane. The electrolytes were then sandwiched between **S1** and ITO/glass, then weight was placed over the device to insure proper contact (**Figure 4**a). Color switch from the initial state to the reduce states were recorded simultaneously at −3 V, reoxidation occurred at +1 V. As expected, the device switched from the initial orange color to dark blue at the LiTFSI-EMITFSI side and to cyan at the EMITFSI side and then back to the orange state at the two sides. To characterize the device color change, the chromaticity parameters ($L^*a^*b^*$) were recorded at each step. These parameters were used to calculate the optical contrast (ΔE^*) (Equation (1)) representing the difference of chromaticity between the initial state and reduced states. In LiTFSI-EMITFSI this optical contrast reaches 43.9, whereas in EMITFSI a ΔE^* of 29.8 is calculated (Figure 4b). In both cases, ΔE^* is far higher than 10 which is the required value to distinguish two color states for the human eye. The optical contrast (ΔE^*) is calculated from $L^*a^*b^*$ parameters as follows:

$$\Delta E^* = \sqrt{\left(L^*_{ox} - L^*_{red}\right)^2 + \left(a^*_{ox} - a^*_{red}\right)^2 + \left(b^*_{ox} - b^*_{red}\right)^2} \quad (1)$$

Interestingly, the stability in EMITFSI was enhanced in the device compared to the solution studies. Devices being closer to conditions of applications, this behavior is encouraging for

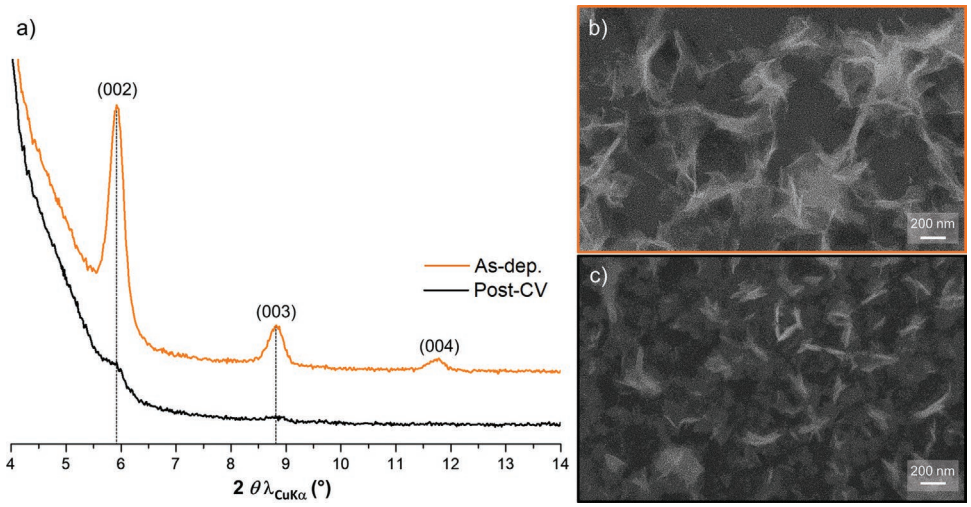

Figure 3. a) Out-of-plane XRD patterns of as-deposited **S1** film and after CV in LiTFSI-EMITFSI. Top view SEM picture of the film b) before and c) after cycling 5 times in LiTFSI-EMITFSI.

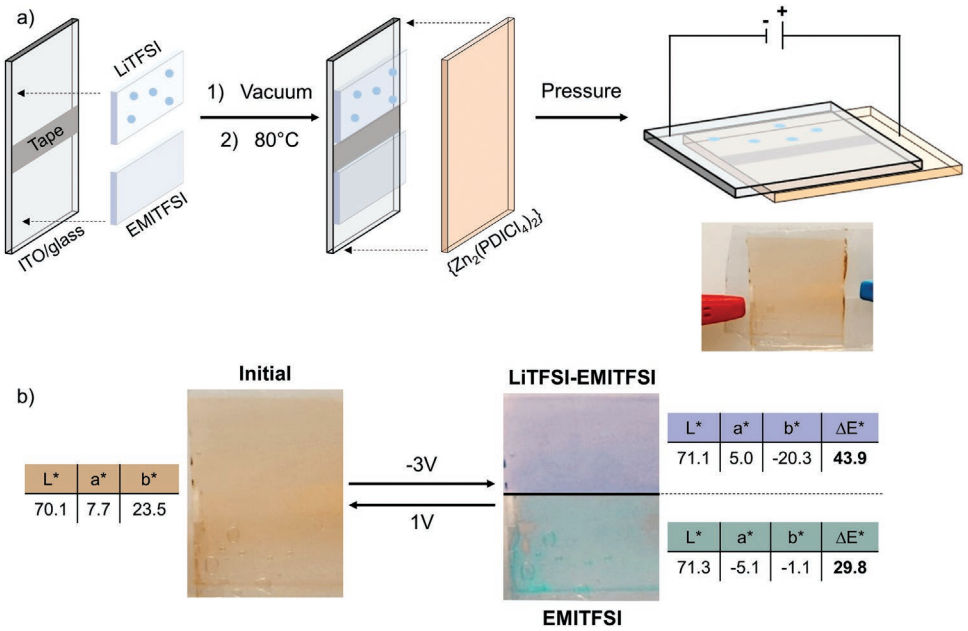

Figure 4. a) Scheme representing the construction of the bi-electrolyte device with a picture of the final device. b) Pictures of **S1**/LiTFSI-EMITFSI+EMITFSI/ITO device showing the initial color and reduced color states with L*a*b parameters and ΔE^* values.

further work with various electrolytes even when the stability in solution is limited. Additionally, the original two-electrolyte configuration of the device opens up new perspectives for electrochromic displays and further work will be consecrated to optimize this proof of concept.

3. Conclusion

In summary, highly oriented electrochromic thin films of $\{Zn_2(PDICl_4)_2\}$ were grown along the (001) axis at room temperature and were characterized by out-of-plane XRD diffraction. Electrochromic properties were investigated in ionic liquids by cyclic voltammetry and spectroelectrochemistry. Two reduced color states were obtained depending on electrolyte composition. Because of the innate porosity of SurMOFs and the affinity of $PDICl_4$ ligands toward Li^+, the commonly blue colored associated with PDI/Li salts solution was highlighted for the first time in the solid state in LiTFSI-EMITFSI. In this medium, good electrochemical stability was achieved. In EMITFSI, a cyan color was obtained by reduction. This optical state matches with the one observed on radical dianions of PDI with a structure close to our ligand, supporting the formation of $PDICl_4$ dianions within the SurMOFs. However, poor electrochemical stability was observed in EMITFSI, leading to the desorption of the film after one or two CV cycles. Interestingly, the stability in solution was greatly improved by methylating the C2 position of the imidazolium. Also, cycling in membrane based electrolyte circumvents the delamination issue. Being closer to conditions for applications, a device composed of the two electrolytes was designed and the two reduced color states were observed simultaneously at −3 V starting from a single orange SurMOF thin film. Additional work is currently ongoing to better characterize the species formed during the reduction of the SurMOF in LiTFSI-EMITFSI and in EMITFSI.

To our knowledge, this work represents the first one regarding the use of SurMOF for electrochromic applications. The unusual color modulation depending on electrolyte composition leads to nonconventional devices. Even though, mechanism is not clear yet, those first results are encouraging for future investigation of SurMOF-based electrochromic thin films and devices. Because of their versatility, SurMOFs offer an infinite amount of electrochromic systems. Electrochromic properties can arise from one or more ligands but also from the metal source. In both cases, this would increase the spectral range reachable with ECDs. In addition, SurMOFs synthesis are compatible with various conductive surfaces (ITO/PET, Au-SAMS...) and are applicable on large areas, widening even more the range of applications of SurMOF-based ECDs.

Supporting Information

Supporting Information is available from the Wiley Online Library or from the author.

Acknowledgements

The authors acknowledge Dr. Fabrice Odobel and Dr. Stéphane Diring (University of Nantes) who provided the perylene diimide ligands. The authors also thank Ambreen Ambreen, Lionel Teulé-Gay, Mathieu Duttine, and Eric Lebraud (ICMCB) for assistance in coloration efficiency calculation, profilometry, EPR and XRD. They would also like to share their gratitude to Brandon Faceira for his help with the optical measurements and fruitful discussion and Jacob Olchowka for ionic

liquids discussion. Finally, they thank Philippe Legros and Nithavong Cam from Placamat for SEM and TOF-SIM.

Conflict of Interest

The authors declare no conflict of interest.

Data Availability Statement

The data that support the findings of this study are available from the corresponding author upon reasonable request.

Keywords

electrochromism, ionic liquids, metal–organic frameworks, surface-anchored metal–organic frameworks, thin films

Received: December 8, 2022
Revised: January 20, 2023
Published online:

[1] O. Shekhah, J. Liu, R. A. Fischer, C. Wöll, *Chem. Soc. Rev.* **2011**, *40*, 1081.
[2] R. A. Fischer, C. Wöll, *Angew. Chem., Int. Ed.* **2009**, *48*, 6205.
[3] D. Zacher, O. Shekhah, C. Wöll, R. A. Fischer, *Chem. Soc. Rev.* **2009**, *38*, 1418.
[4] O. Shekhah, H. Wang, M. Paradinas, C. Ocal, B. Schüpbach, A. Terfort, D. Zacher, R. A. Fischer, C. Wöll, *Nat. Mater.* **2009**, *8*, 481.
[5] D. Li, Y. Tian, Q. Lin, J. Zhang, Z. Gu, *ACS Appl. Mater. Interfaces* **2022**, *14*, 33548.
[6] S. Begum, T. Hashem, M. Tsotsalas, C. Wöll, M. H. Alkordi, *Energy Technol.* **2019**, *7*, 5.
[7] A. Jaafar, S. El-Husseini, C. Platas-Iglesias, R. A. Bilbeisi, *J. Environ. Chem. Eng.* **2022**, *10*, 108019.
[8] H. J. Park, M. C. So, D. Gosztola, G. P. Wiederrecht, J. D. Emery, A. B. F. Martinson, S. Er, C. E. Wilmer, N. A. Vermeulen, A. Aspuru-Guzik, J. F. Stoddart, O. K. Farha, J. T. Hupp, *ACS Appl. Mater. Interfaces* **2016**, *8*, 24983.
[9] C. G. Granqvist, *Sol. Energy Mater. Sol. Cells* **2000**, *60*, 201.
[10] P. M. Beaujuge, J. R. Reynolds, *Chem. Rev.* **2010**, *110*, 268.
[11] H. W. Heuer, R. Wehrmann, S. Kirchmeyer, *Adv. Funct. Mater.* **2002**, *12*, 89.
[12] J. Seidel, W. Luo, S. J. Suresha, P. K. Nguyen, A. S. Lee, S. Y. Kim, C. H. Yang, S. J. Pennycook, S. T. Pantelides, J. F. Scott, R. Ramesh, *Nat. Commun.* **2012**, *3*, 799.
[13] C. R. Wade, M. Li, M. Dincă, *Angew. Chem., Int. Ed.* **2013**, *52*, 13377.
[14] I. Mjejri, C. M. Doherty, M. Rubio-Martinez, G. L. Drisko, A. Rougier, *ACS Appl. Mater. Interfaces* **2017**, *9*, 39930.
[15] K. Takada, R. Sakamoto, S. T. Yi, S. Katagiri, T. Kambe, H. Nishihara, *J. Am. Chem. Soc.* **2015**, *137*, 4681.
[16] W. Ma, L. Qin, Y. Gao, W. Zhang, Z. Xie, B. Yang, L. Liu, Y. Ma, *Chem. Commun.* **2016**, *52*, 13600.
[17] W. Zhang, X. Zhou, Z. Xie, B. Yang, L. Liu, Y. Ma, *Chem. Commun.* **2013**, *49*, 11560.
[18] Z. Chen, M. G. Debije, T. Debaerdemaeker, P. Osswald, F. Würthner, *ChemPhysChem* **2004**, *5*, 137.
[19] R. Haldar, A. Mazel, R. Joseph, M. Adams, I. A. Howard, B. S. Richards, M. Tsotsalas, E. Redel, S. Diring, F. Odobel, C. Wöll, *Chem. – Eur. J.* **2017**, *23*, 14316.
[20] R. Haldar, S. Diring, P. K. Samanta, M. Muth, W. Clancy, A. Mazel, S. Schlabach, F. Kirschhöfer, G. Brenner-Weiß, S. K. Pati, F. Odobel, C. Wöll, *Angew. Chem., Int. Ed.* **2018**, *57*, 13662.
[21] R. Haldar, M. Jakoby, A. Mazel, Q. Zhang, A. Welle, T. Mohamed, P. Krolla, W. Wenzel, S. Diring, F. Odobel, B. S. Richards, I. A. Howard, C. Wöll, *Nat. Commun.* **2018**, *9*, 4332.
[22] J. Liu, B. Lukose, O. Shekhah, H. K. Arslan, P. Weidler, H. Gliemann, S. Bräse, S. Grosjean, A. Godt, X. Feng, K. Müllen, I. B. Magdau, T. Heine, C. Wöll, *Sci. Rep.* **2012**, *2*, 921.
[23] S. Seifert, D. Schmidt, F. Würthner, *Chem. Sci.* **2015**, *6*, 1663.
[24] V. Monnier, F. Odobel, S. Diring, *Chem. Commun.* **2022**, *58*, 9429.
[25] M. Da Rocha, B. Dunn, A. Rougier, *Sol. Energy Mater. Sol. Cells* **2019**, *201*, 110114.
[26] A. Danine, L. Manceriu, C. Faure, C. Labrugère, N. Penin, A. Delattre, G. Eymin-Petot-Tourtollet, A. Rougier, *ACS Appl. Mater. Interfaces* **2019**, *11*, 34030.